

# In-Vivo and In-Vitro Measurements of Lead and Cadmium

DAVID R. CHETTLE,\* DIANA M. FRANKLIN,  
CHARLES J. G. GUTHRIE, MALCOLM C. SCOTT,  
AND LILLIAN J. SOMERVILLE

*Department of Physics, University of Birmingham, England.*

## ABSTRACT

Tibia lead is measured in vivo using X-ray fluorescence. A  $^{109}\text{Cd}$  source is used to excite Pb K X-rays, and this signal is normalized to that from Rayleigh scattering to remove geometrical variations. The lower limit of detection is  $10\ \mu\text{g/g}$  for a mean absorbed dose, to the exposed section of the leg, of  $100\ \mu\text{Gy}$ . Tibia lead correlated positively with age in normal volunteers ( $r = 0.615$ ,  $p = 0.004$ ) and with duration of exposure in occupationally exposed subjects ( $r = 0.847$ ,  $p = 0.0001$ ). When the X-ray fluorescence technique was applied to autopsy specimens previously analyzed by atomic absorption spectrometry there was excellent agreement between measurement techniques.

Cadmium is measured in vivo by neutron activation analysis. The detection limit in liver is  $6.5\ \mu\text{g/g}$  for a local skin dose equivalent of  $0.5\ \text{mSv}$  and in kidney is  $6.4\ \text{mg}$  for a dose equivalent of  $0.9\ \text{mSv}$  to the skin. Detailed analysis of the  $\gamma$ -ray spectrum will produce only slight improvements in detection limit. Uncertainties in organ position during measurement, even after ultrasonic localization, are likely to produce uncertainties of 20–25% in cadmium measurement. Autopsy samples were measured, using a fast neutron activation method, from people previously measured in vivo. The results are broadly consistent, but show differences greater than those accounted for by counting statistics.

**Index Entries:** In vivo bone lead measurement, and  $^{109}\text{Cd}$ ; in vivo bone lead measurements, and Rayleigh scattering; in vivo X-ray fluorescence; in vivo liver and kidney cadmium measurement; in vivo

\*Author to whom all correspondence and reprint requests should be addressed. Element Research Vol. 11, 1986.

neutron activation analysis; comparisons of in vivo and in vitro data;  
 $\gamma$ -ray spectral analysis.

## INTRODUCTION

Since both lead and cadmium have relatively long residence times in some organs of the human body, levels accumulate over periods of years or even decades so that not only are they detectable, but their measurement also provides an indication of cumulative exposure. Clearly, in both these cases, interest in these in vivo measurement data centers around the toxic effects of the two metals. The technique used for lead measurement is energy-dispersive, source-excited X-ray fluorescence (XRF), whereas cadmium is measured by a neutron activation analysis (NAA) technique utilizing  $\gamma$ -rays emitted promptly following thermal neutron capture by  $^{113}\text{Cd}$ .

The in vivo lead measurement system described here is that developed at Birmingham, which has favorable performance characteristics in terms of detection limit (10  $\mu\text{g/g}$ ) and dose to the subject (100  $\mu\text{Gy}$ ). The results of some studies of industrially exposed people are presented and contrasted with those from people whose only exposure to lead is through the general, urban environment. Data from the use of this XRF technique to measure the lead content of autopsy samples are then compared with atomic absorption spectrometry results obtained from the same bones. These serve, at least in part, to validate the in vivo measurements.

In vivo cadmium measurements have been undertaken for a decade now, so there are only relatively minor changes in system design and performance to report, together with improvements in spectral analysis. Of more significance to the use of this tool in toxicological research and occupational biological monitoring are inaccuracies associated with organ localization and, more particularly, with slight movements by the subject during the measurement. Recently, autopsy samples have become available from people previously measured in vivo. These have been analyzed using a fast neutron activation technique and compared with the corresponding in vivo results. The data, from a few samples, are broadly consistent, but the variance between analyses is greater than that accounted for by counting statistics, which indicates the importance of positional uncertainties in contributing to inaccuracies in in vivo measurements.

## Pb MEASUREMENTS

Energy-dispersive, source-excited XRF has been used by other laboratories to measure lead in vivo. Ahlgren et al. (1,2) used a  $^{57}\text{Co}$  source to measure lead in finger bones, obtaining a lower limit of detection of 20  $\mu\text{g/g}$  for a dose, at the midpoint of the fingerbone, of 2.5 mGy; at about

the same time, Bloch et al. (3) measured lead in teeth, using the same isotope as a source and achieving broadly similar performance characteristics. More recently, Price et al. (4) have been using a system modeled on that first developed by the Swedish group; all three groups use the K X-rays to measure lead concentration. In contrast to this, Wielopolski et al. (5) have used lower energy sources, silver K X-rays from  $^{109}\text{Cd}$  or tellurium K X-rays from  $^{125}\text{I}$ , to excite the lead L X-rays in tibia. The resulting detection limit is comparable with the other systems, but the dose, 10 mGy, is somewhat larger, although the mass of tissue irradiated is appreciably smaller.

### $^{109}\text{Cd}$ Technique

In Birmingham we opted for tibia as the measurement site, taking it to be a characteristically cortical bone. Initially we examined  $^{57}\text{Co}$  as a source, but concluded that  $^{109}\text{Cd}$  was likely to prove preferable (6). Subsequent work (7) showed that a satisfactory measurement could be made in this way. A full description of the technique has recently been reported (8), and it will only be summarized briefly here.

The  $^{109}\text{Cd}$  emits  $\gamma$ -rays, in 3.6% of decays, of 88.035 keV, which are only 30 eV above the lead K absorption edge. These  $\gamma$ -rays therefore have a high cross-section for photo-electric interaction with lead, which assists measurement sensitivity. Another feature of the use of this source is that photons undergoing Compton scattering through relatively large angles have energies between 65.5 and 67.5 keV, well clear of the lead K X-rays at 72.8 and 75.0 keV. This feature makes for a large characteristic signal to Compton continuum ratio, which in turn enhances sensitivity. The experimental arrangement is outlined in Fig. 1. An annular  $^{109}\text{Cd}$  source ( $\sim 5$  GBq, Amersham International type CUCQ 8206) is mounted in front of and coaxially with a planar hyperpure germanium detector (Ortec type 1113-16220-S), which has a resolution (fwhm) of 480 eV and efficiency of 50% at 75 keV. The source-detector assembly is positioned so that the midpoint of the subject's tibia is axially in front of it, and the source to skin distance is 30 mm. A spectrum from a high-lead-doped plaster-of-paris cylinder is shown in Fig. 2. This shows the separation of the lead K X-rays from the Compton scattered peak; it also shows a fairly prominent, coherently scattered peak from the 88 keV source photons. For the range of angles used here (140–170°) and at this energy the coherent scattering cross-section is very strongly dependent on atomic number ( $Z^5$ – $Z^7$ ) (9), and, thus, the feature we observe comes almost entirely from the bone mineral. Since lead is also very strongly concentrated in bone, the ratio of lead X-ray counts to coherent counts is very nearly independent (> 99%) of the measurement geometry. The value of this effect is illustrated in Fig. 3, which shows the variation of lead counts with the amount of soft tissue overlying a bone phantom and how this variation is eliminated when lead counts are normalized to coherent counts. It should be

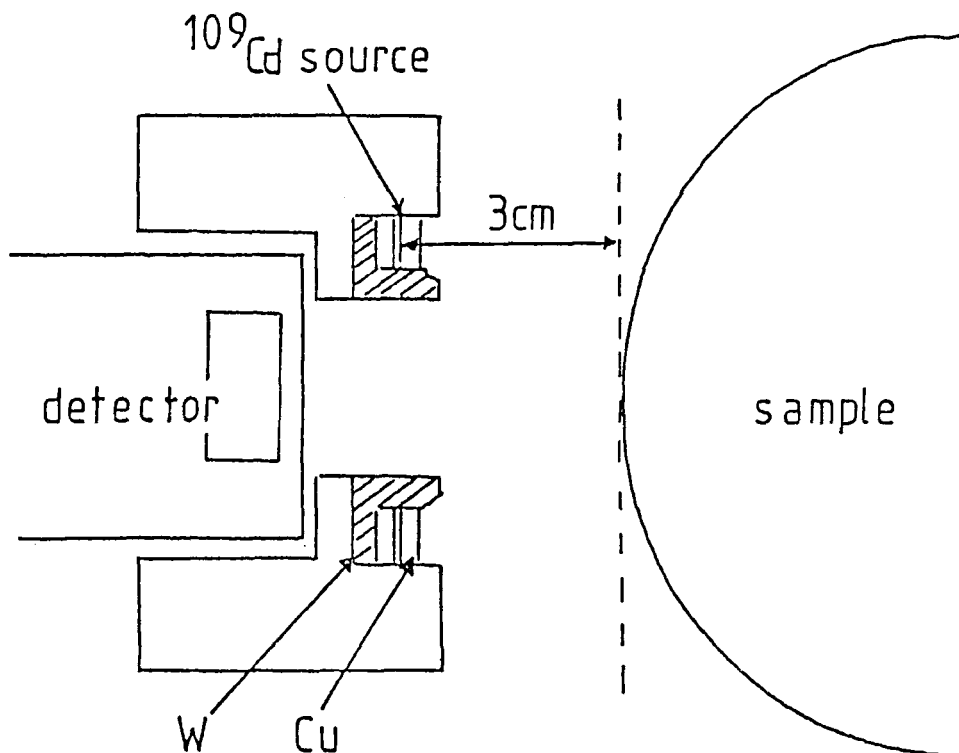


Fig. 1. Source-sample-detector arrangement for in vivo lead measurements.

noted, however, that the sensitivity is worse for obese subjects with large amounts of overlying tissue. This normalization has also been shown to remove the variation caused by differences in source-to-sample distance, phantom shape, and bone marrow cavity (8).

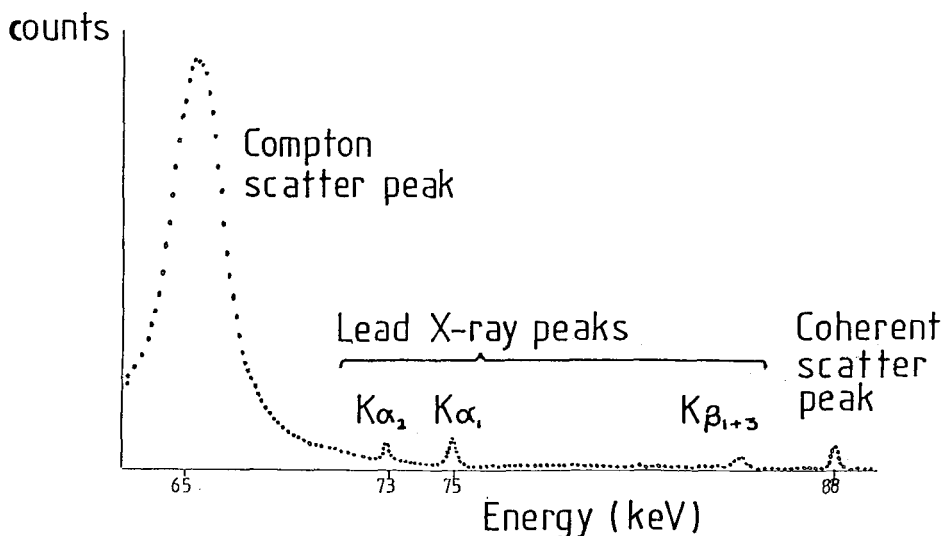


Fig. 2. X-ray-fluorescence spectrum from 1000 µg/g lead.

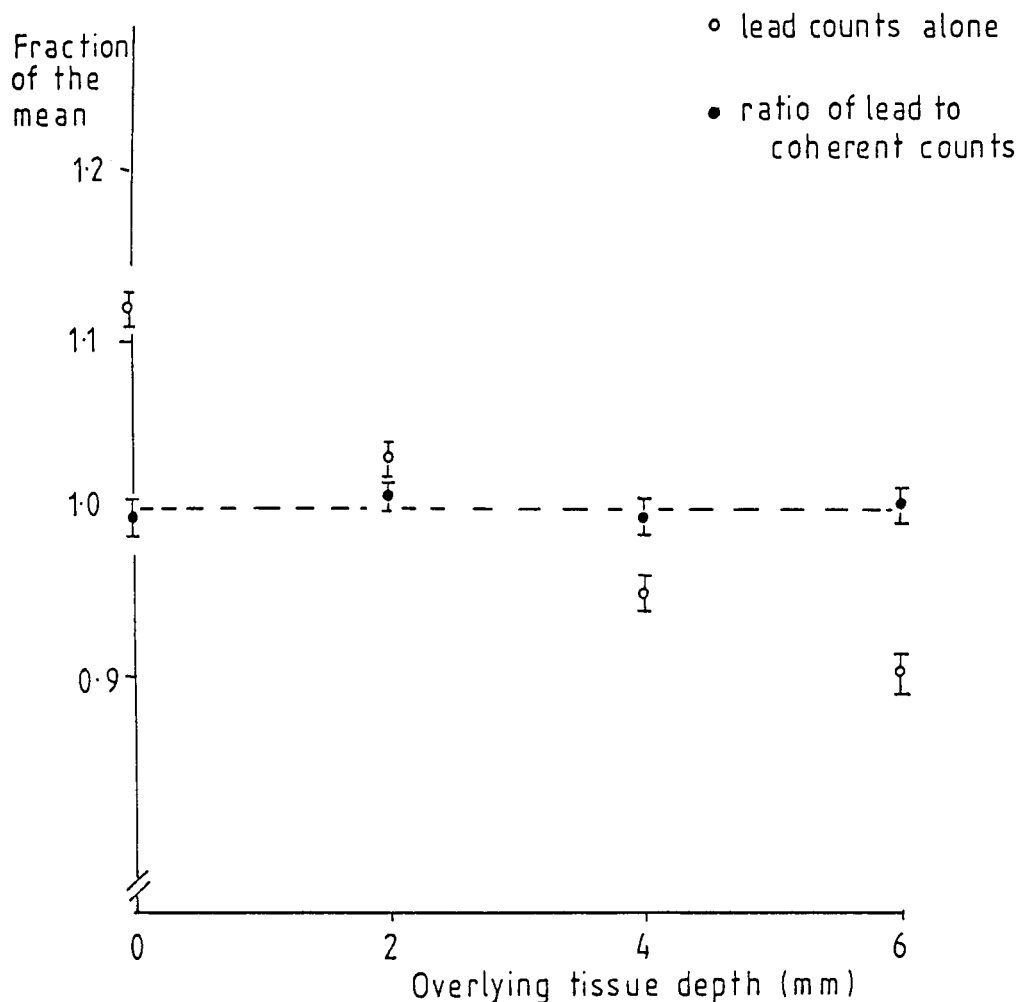


Fig. 3. Variation of lead counts, and lead counts normalized to coherent counts, with overlying tissue.

Using this experimental arrangement, a lower level of detection of 10  $\mu\text{g Pb/g}$  bone is obtained for a dose of 100  $\mu\text{Gy}$ . The detection limit used here is defined as that lead concentration that produces a peak that has a net area,  $P$ , equal to twice its standard error ( $\sigma_P$ ). Thus,  $P = 2\sigma_P$ , and we note that  $\sigma_P$  tends to  $(2^{1/2} \times \sigma_B)$  as  $P$  tends to zero, where  $\sigma_B$  is the standard error of the background underlying the peak. This criterion,  $2\sigma_P$ , is thus  $(8/9)^{1/2} \times 3\sigma_B$ , where  $3\sigma_B$  is the criterion that a peak be three times the standard error of the background. In our case, the detection limit would remain 10  $\mu\text{g/g}$  on the  $3\sigma_B$  criterion, since the value had been rounded up somewhat to achieve a conservative estimate. The dose quoted is an average over a 20-cm section of the calf, involving a mass of 1.5–2.0 kg of tissue, this represents the volume of tissue within which 90% of the energy imparted during the measurement is absorbed. This calculated dose was cross-checked, not only against thermoluminescent

dosimetry, but also against a Monte Carlo simulation (10). The Monte Carlo program was originally written to study the factors determining the shape of the detected photon energy distribution, and it achieved good agreement between predicted and observed spectra (6). The results of all three dose estimates agreed quite closely on a figure of about 65  $\mu\text{Gy}$ , and the 100  $\mu\text{Gy}$  we quote represents an upper limit to the dose delivered. As can be seen, the performance of this  $^{109}\text{Cd}$  system compares favorably with alternative approaches to this sort of *in vivo* measurement of lead. So, having obtained ethical approval, we were able to proceed to make measurements on a number of normal volunteers and on some people specifically exposed to lead at their place of work.

### ***In Vivo Lead Data***

Previous autopsy studies show that tibial lead concentrations tend to increase with age, ranging up to 30  $\mu\text{g/g}$  or so (11). Figure 4 shows the tibial lead values we have observed for 20 normal volunteers, mostly drawn from members of the University, plotted against their age. A number of these measurements fall below the detection limit of 10  $\mu\text{g/g}$ , but the technique is nevertheless sufficiently precise to show a similar trend to that reported by Barry; and the correlation between tibia lead and age was significant ( $r = 0.615$ ,  $p = 0.004$ ).

When a group of 15 people, who work at the same factory handling lead, was measured it was immediately clear that their lead levels were significantly raised, reflecting their contaminated working environment. In this group, tibia lead correlated quite strongly ( $r = 0.857$ ,  $p < 0.0001$ ) with the number of years each person had worked at the factory, despite the fact that such a simple index of cumulative exposure would be expected to be rather imprecise.

The time taken for each measurement was between 15 and 30 min, depending on the source strength. The subject was seated in a converted dental chair in reasonable comfort, and the measurement technique proved itself to be very acceptable to the people concerned, straightforward from the operator's point of view and quite readily transported to a factory site and set up there.

### ***In Vitro Comparisons***

Some studies of autopsy bone samples were undertaken, partly to show the application of the XRF technique in a somewhat different situation, but principally as a further cross-check on the *in vivo* measurements. Nine bone sections, samples of which had previously been analyzed by atomic absorption spectrometry (AAS) (12,13), were supplied to us by Dr. Arthur C. Aufderheide, of the University of Minnesota-Duluth. These comprised a section of tibia and two metatarsals from each of three people. The autopsy specimens were analyzed using the same apparatus employed for the *in vivo* studies, with lead counts being normalized to

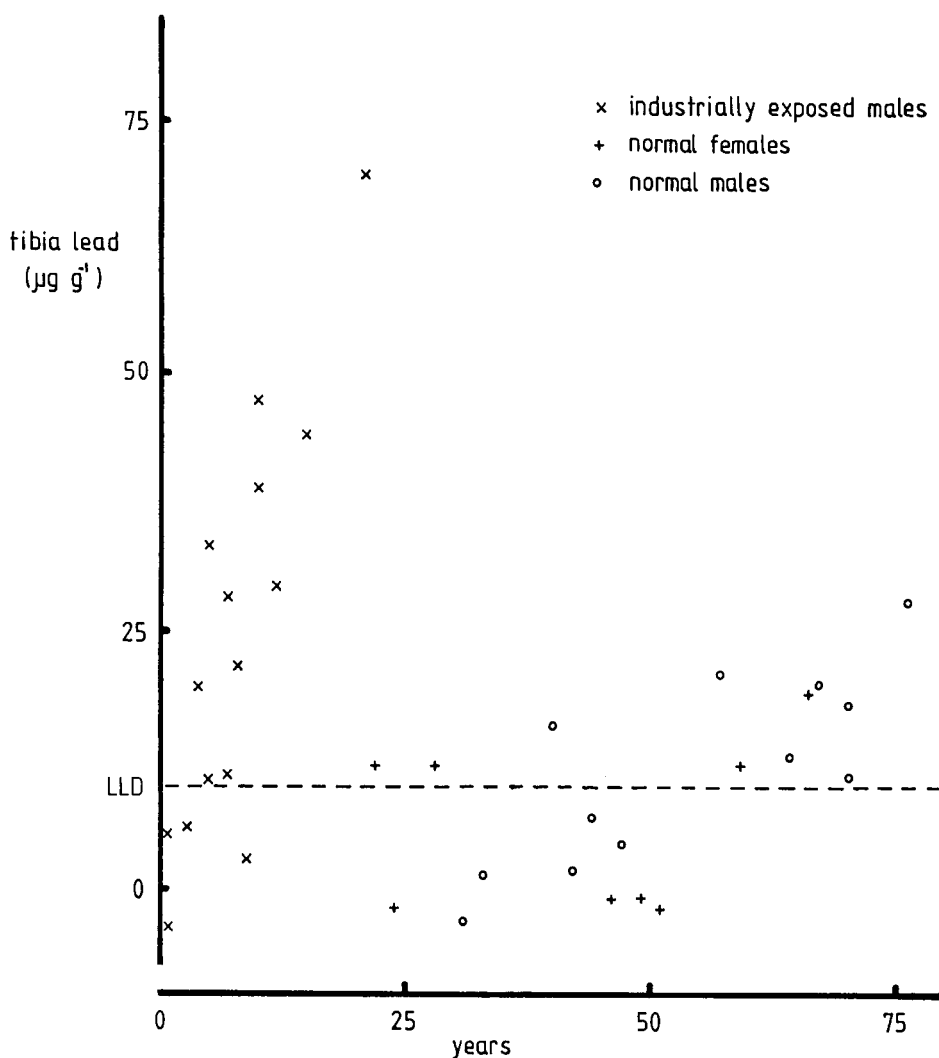


Fig. 4. Variation of tibia lead with age for normals and with years exposure for industrial workers. The tibia lead value for industrially exposed workers is the observed level minus the expected value for a person of that age. The lower limit of detection (LLD) is also indicated.

coherent counts in the same way. In this case the sample size and shape varied considerably (between tibia and metatarsal), so the comparison with AAS measurements provided a further test of the robustness of the coherent correction. The histogram in Fig. 5 shows a comparison of the XRF with the AAS results. As can be seen, there is no evidence of a systematic difference between the techniques. In fact, the mean difference,  $d_i$ , between paired analyses was  $<1 \mu\text{g/g}$  ( $d_i = 0.8 \pm 5.8$ ) and was not significantly different from zero.

We conclude, therefore, that the XRF technique for in vivo lead measurements described here provides a simple, reliable, low-dose means of estimating lead stored, in this case, in one of the major cortical

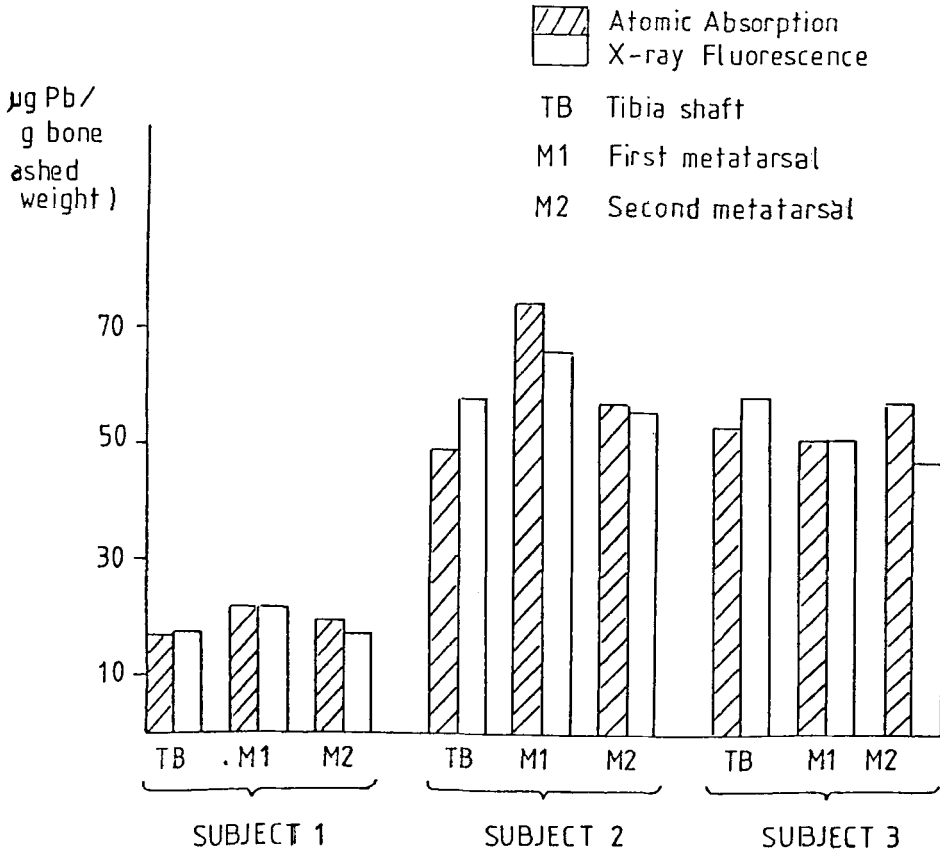


Fig. 5. Comparison of X-ray fluorescence and atomic absorption spectroscopy results.

bones of the body. It seems likely that the data thus generated will contribute toward an understanding of the longer-term health effects related to lead exposure and may, in time, find a role within the biological monitoring of occupational exposure to this metal.

## Cd MEASUREMENTS

The feasibility of making *in vivo* cadmium measurements by counting  $\gamma$ -rays emitted promptly following neutron capture by  $^{113}\text{Cd}$  was mentioned by Biggin et al. (14), and *in vivo* measurements of human liver cadmium were reported a decade ago (15). This prompt  $\gamma$ -ray NAA technique has now been adopted, with a number of significant variations, by several laboratories around the world (16–20). In addition, an XRF technique based at first on  $^{241}\text{Am}$  (21) and later using the polarized output of an X-ray tube to excite Cd X-rays (22) has been developed by the group working at Malmö in Sweden. At Birmingham we measure cadmium both in the liver and during a separate measurement in the left kidney, using either the Nuffield cyclotron (15,23) or  $^{238}\text{Pu}/\text{Be}$  sources to



provide fast neutrons (24,25). Fast neutrons are collimated to irradiate the appropriate portion of the body; they are slowed, largely by elastic scatter, and can then undergo capture in various elements. The macroscopic cross-section for thermal neutron capture can be significant, despite the low-number density of cadmium nuclei, because of the unusually large capture cross-section of the 12.26% abundant  $^{113}\text{Cd}$  (19,910 b).  $\gamma$ -Rays from this and other reactions are detected in large volume Ge semiconductors, and the most prominent line from cadmium, at 559 keV, is used to quantify the elemental content. The majority of measurements we make use the  $^{238}\text{Pu}/\text{Be}$  based systems, since these can be transported to factories so that the work force can be monitored on site. The present system for liver measurements is shown schematically in Fig. 6 and is very similar to that reported by Scott et al. (26), except that LiF has been replaced by  $\text{B}_2\text{O}_3$  in the shielding assembly. The kidney-measurement system is a scaled up version of that used for liver, and it uses 1.5 TBq of  $^{238}\text{Pu}/\text{Be}$ , rather than 0.37 TBq in the liver system, and two detectors rather than one. In a recent survey the detection limit for cadmium in liver was 6.5  $\mu\text{g}/\text{g}$  [2 standard errors of (gross peak - background) or 4.6  $\mu\text{g}/\text{g}$ , 2 standard errors of background] and that in kidney was 6.4 mg (4.5 mg, 2 standard errors of background). The dose equivalent to the skin (neutron +  $\gamma$ -ray) was 0.5 mSv for the liver and 0.9 mSv for the kidney measurement.

### $\gamma$ -Ray Spectrum Fitting

A portion of the  $\gamma$ -ray spectrum (from about 500 to about 600 keV), representative of that obtained during an in vivo liver cadmium measurement, is shown in Fig. 7. In this case the cadmium peak, which corresponds to 10  $\mu\text{g}/\text{g}$ , is not very distinctive, and its analysis is complicated by the nearby feature at 563 keV. This feature, with its characteristic higher-energy tail, arises from fast neutron inelastic scattering off  $^{76}\text{Ge}$  in the detector itself. Until now a simple spectrum analysis procedure has been used; this involved fitting a straight line to those portions of the  $\gamma$ -ray spectrum between 500 and 600 keV, which were relatively free of specific features. In an attempt to improve precision, a more specific spectral analysis approach has been investigated. The portion of the spectrum that included the peak from  $^{114}\text{Cd}$  and that from  $^{76}\text{Ge}$  was fitted by the function:

$$Y = A_1 + A_2X + A_3 \left\{ \exp \left[ -\frac{1}{2} \frac{X - A_4}{C_1} \right] + C_2 \right\} \\ + A_5 \left\{ \frac{1}{2} + \frac{1}{\pi} \arctan \left[ \frac{X - (A_4 + C_3)}{C_4} \right] \right\} + f$$

using a nonlinear least squares algorithm developed by Marquardt (27) and reported in the form of a Fortran program by Bevington (28). In the above expression,  $Y$  is the channel content,  $X$  is the channel number,  $A_i$

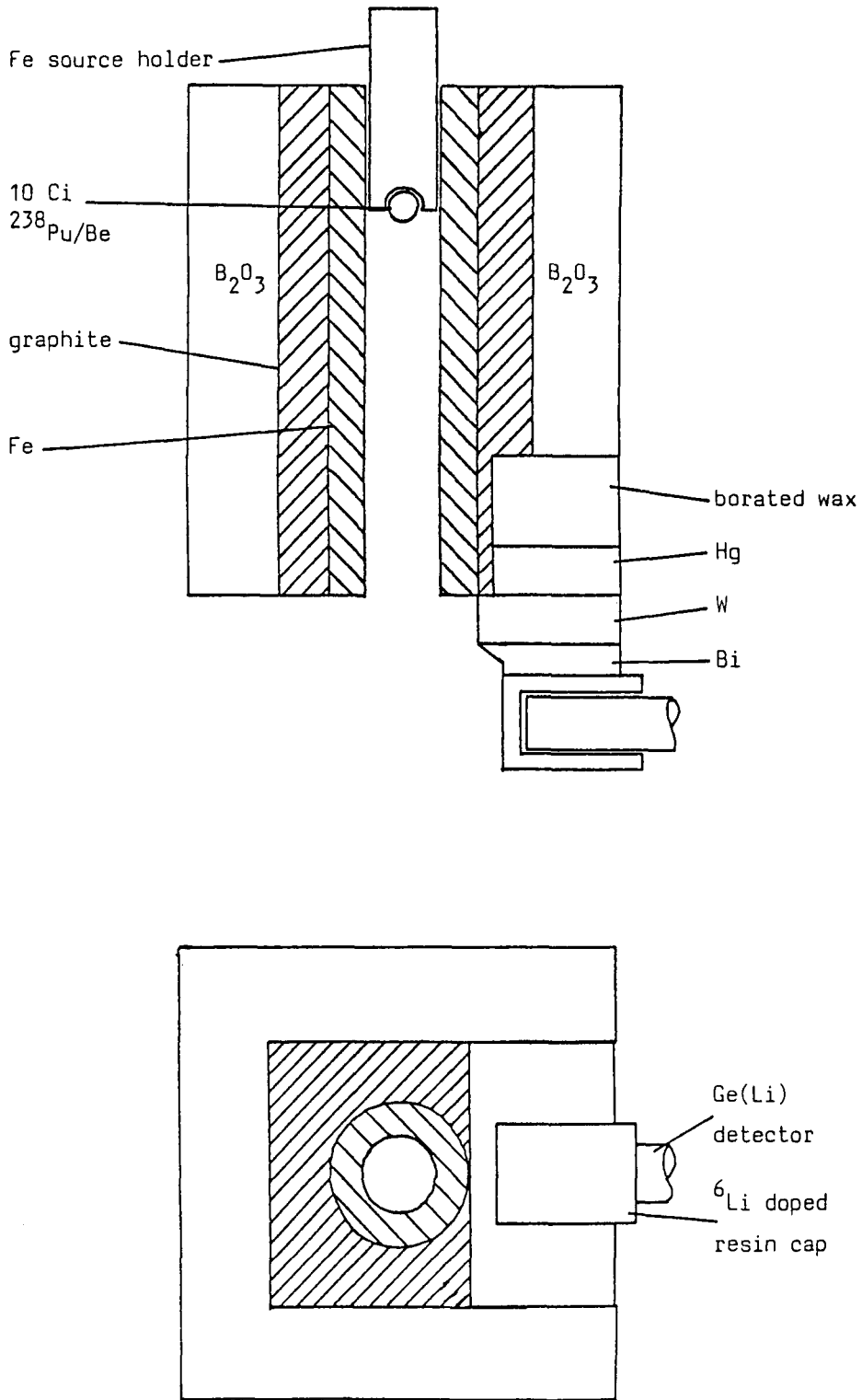


Fig. 6. Liver cadmium measurement system. (Top) sectional view. (Bottom) front view.

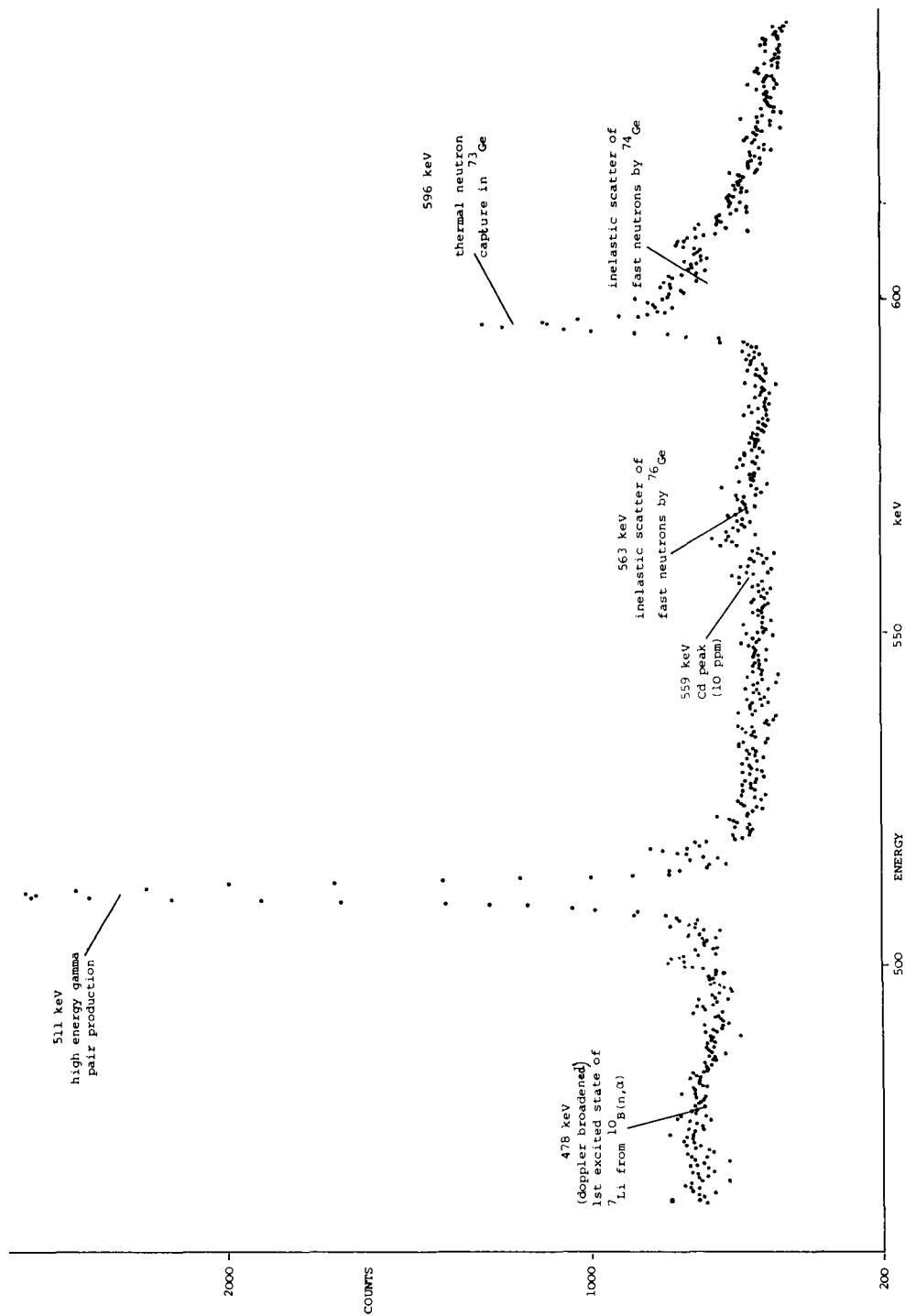


Fig. 7.  $\gamma$ -Ray energy spectrum from 10  $\mu\text{g/g}$  cadmium phantom.

are the parameters that are adjusted to obtain the best fit to the observed data and  $C_i$  are parameters that are treated as constant from one spectrum to another;  $C_2 = 0$  for  $X > A_4$  and  $= 0.028$  for  $X < A_4$ ,  $f = \exp(A_6 X)$  for  $X > (A_4 + C_3)$  and  $= 1$  for  $X < (A_4 + C_3)$ .

The result of such a fit to a 10  $\mu\text{g/g}$  liver cadmium phantom is shown in Fig. 8. Although this fit is encouragingly good ( $1.0 < \chi^2 < 1.4$ ), the resulting improvement in precision was only marginal (from 6.5 to 6.2  $\mu\text{g/g}$ ), suggesting that the cruder technique used previously was not contributing significantly to the overall measurement uncertainty.

### Positional Uncertainties

The effect of relatively small uncertainties in organ position on the accuracy of these in vivo cadmium measurements has been documented previously (29), as has the use of ultrasonic scanning to locate the organ of interest prior to measurement. The problem is not too great in the case of liver measurements, as can be seen from Fig. 9, which shows a cadmium count vs depth calibration curve generated using a high concentration phantom. Also shown is a histogram showing the distribution of liver depths (distance from skin to nearest surface of liver) observed in a recent survey. Some of the very deep outliers may be incorrectly recorded because of difficulties encountered in obtaining a clear echo from the liver surface, particularly in some subjects who were elderly and obese. A further possible source of inaccuracy, not reflected in the data in Fig. 9, is that some subjects moved during the measurement, which

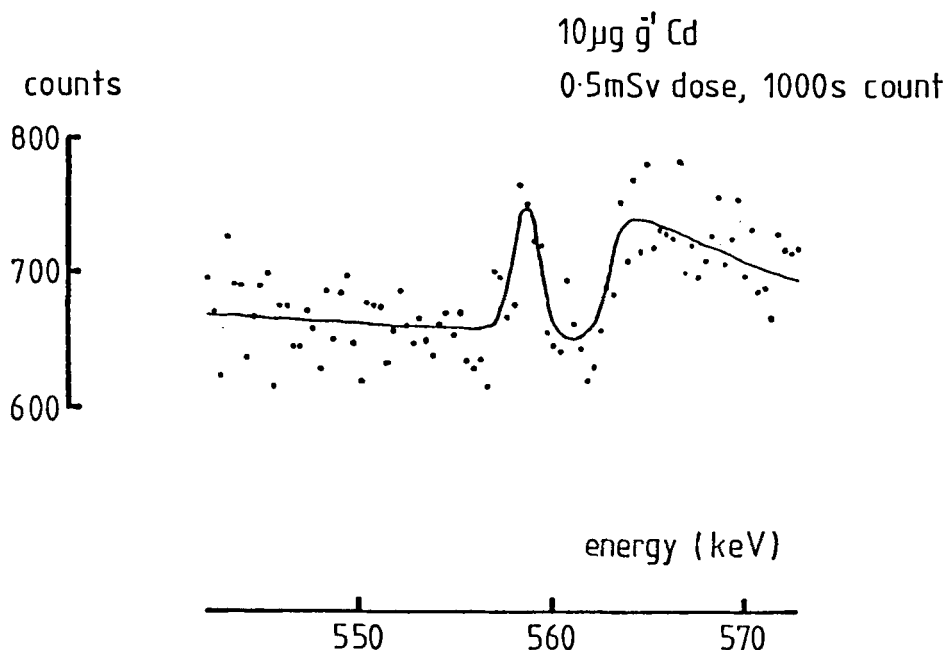


Fig. 8. Cadmium spectrum with fitted function superimposed.

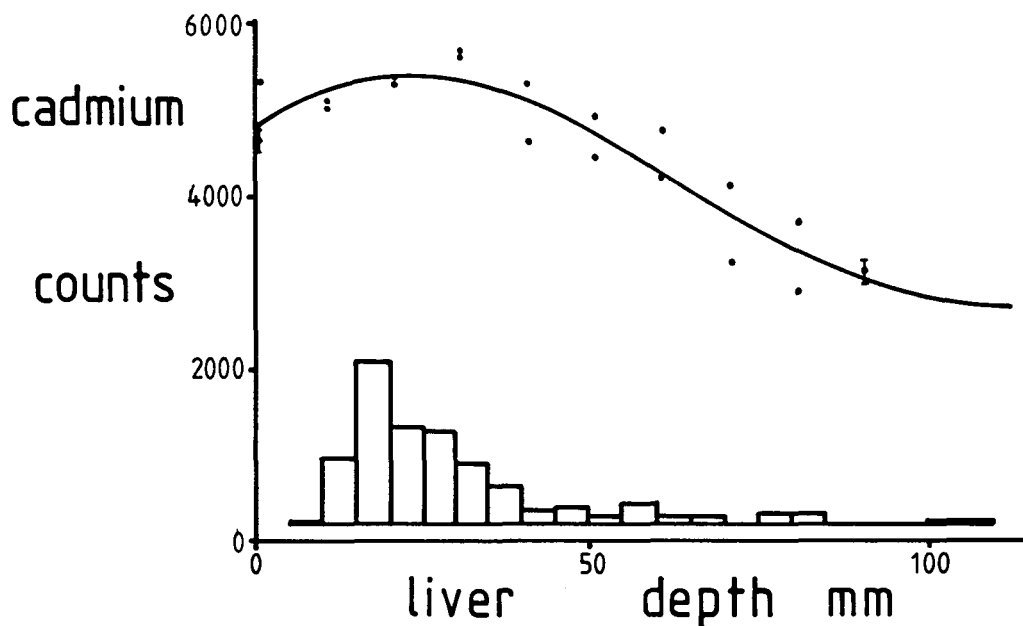


Fig. 9. Liver cadmium depth correction curve; histogram shows distribution of observed liver depths.

takes about 20 min. A subject is seated facing the liver-system collimator, and we have observed a tendency for some people to slump backward. When this occurs, the liver is moved away from both the neutron source and the detector. Inaccuracies in kidney cadmium measurements are likely to be more severe than in the case of liver; this is illustrated by Fig. 10, which shows a kidney cadmium depth correction curve and the distribution of observed kidney depths. Here the range of correction factors that have to be applied to in vivo data is large, and even the spread in data generated by the phantom measurements is substantial. This emphasizes the extent to which our present measurement geometry is sensitive to minor positional uncertainties. Problems of movement during a measurement are less important in the case of kidney. Earlier work (30) showed that the bulk motion of the kidney caused by breathing was much less for a seated person than for someone lying down, and we have observed that people remain close to their original position during measurement.

We concluded that we need to be cautious in the accuracy claimed for in vivo measurements and have tentatively assigned positional uncertainties of  $\pm 20\%$  to liver data and  $\pm 25\%$  to kidney data. Meanwhile, we are actively investigating other measurement geometries, looking for an arrangement that would be appreciably less sensitive to uncertainties in organ position. It should be noted that this lack of accuracy does not preclude valid and useful interpretation of cadmium data. For people with relatively low cadmium burdens, the overall measurement uncertainty is still dominated by counting statistics; whereas for those who are more

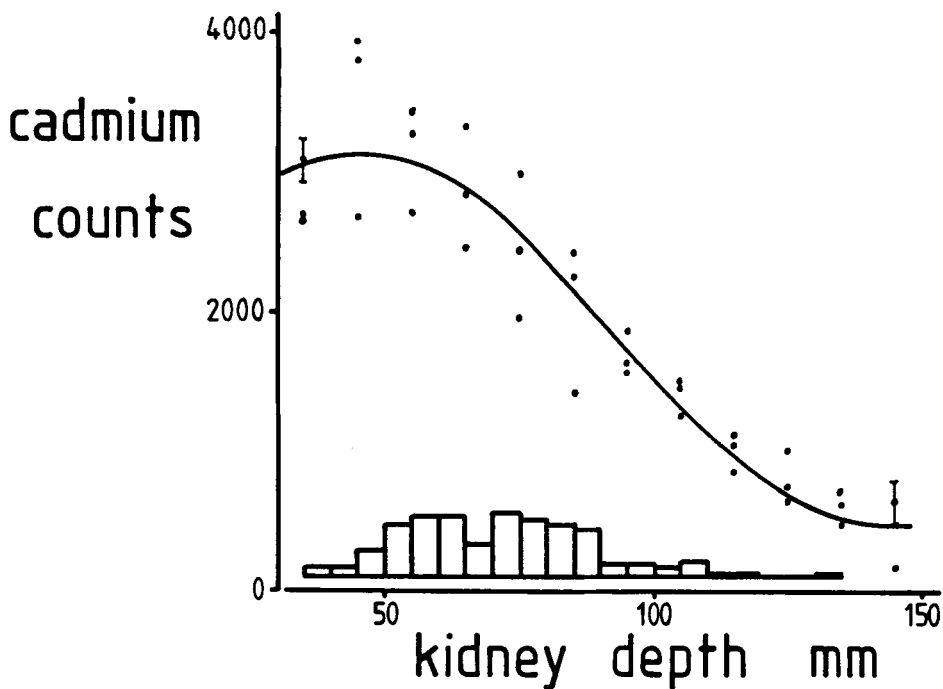


Fig. 10. Kidney cadmium depth correction curve; histogram shows distribution of observed kidney depths.

highly exposed, there is still a clearcut discrimination between their levels and those in a normal population.

### ***Comparison Between In Vivo and In Vitro Data***

When autopsy samples became available from people whom we had previously measured in vivo we approached them with some trepidation, bearing in mind our increasing awareness of the problems of accuracy for in vivo data. In the first case we could only obtain small portions of liver and kidney, but for subsequent cases we were supplied with either whole organs or substantial proportions of them. The cadmium content was assayed using a fast neutron activation technique. Neutrons from a beryllium target, bombarded with 20 MeV deuterons, irradiated the samples, and the activity of  $^{111\text{m}}\text{Cd}$  ( $t_{1/2} = 48.6$  min) was counted. Each of the following three reactions could contribute:  $^{112}\text{Cd}(n,2n)^{111\text{m}}\text{Cd}$ ;  $^{111}\text{Cd}(n,n')^{111\text{m}}\text{Cd}$ ;  $^{110}\text{Cd}(n,\gamma)^{111\text{m}}\text{Cd}$ .

Samples and phantoms were wrapped in a plastic sheet, which in turn was wrapped in cadmium, to reduce interference from thermal neutron reactions in sodium and chlorine. Since cadmium-free phantoms showed no evidence of  $^{111\text{m}}\text{Cd}$  activity, it is clear that this procedure introduced no contamination of the samples. When possible, sample sizes were arranged to be about 100 g and several sets of phantoms were used in order to match varying sample sizes. Livers were measured in a num-

ber of different portions, each of approximately 100 g. Each sample or calibration phantom was irradiated with a high-concentration reference phantom, and these were rotated in the neutron beam during the irradiation, which was typically 1.5 h. The two active specimens were then counted simultaneously on Ge(Li) detectors for about 1.5 h. This procedure is shown in outline in Fig. 11; the intention behind it was to eliminate any uncertainties arising from variations in irradiation or cooling times.  $^{111m}\text{Cd}$  emits  $\gamma$ -rays at 151 and 245 keV, of which the latter is the more prominent and is therefore the one we used in this analysis. A spectrum of the energy region of interest is shown in Fig. 12. The promi-

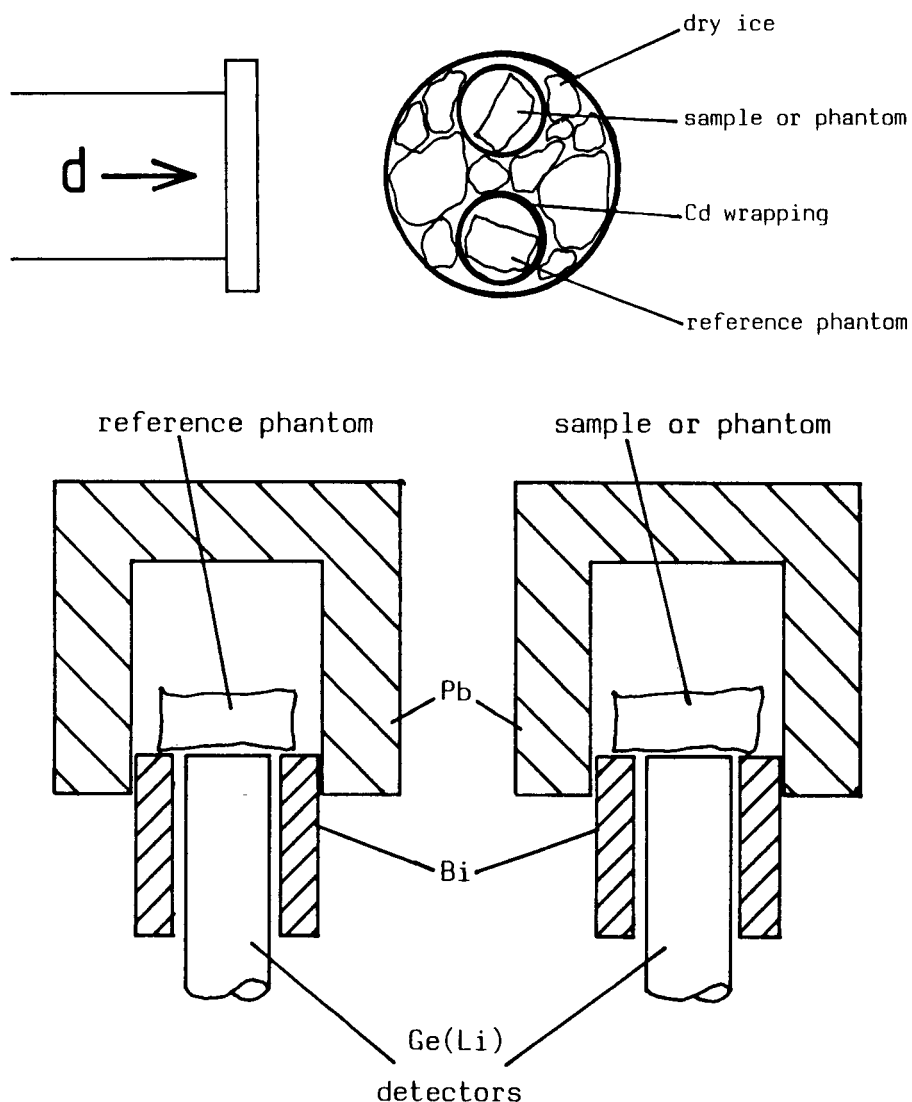


Fig. 11. Outline of procedures for in vitro cadmium analyses: (Top) irradiation; (Bottom) counting.

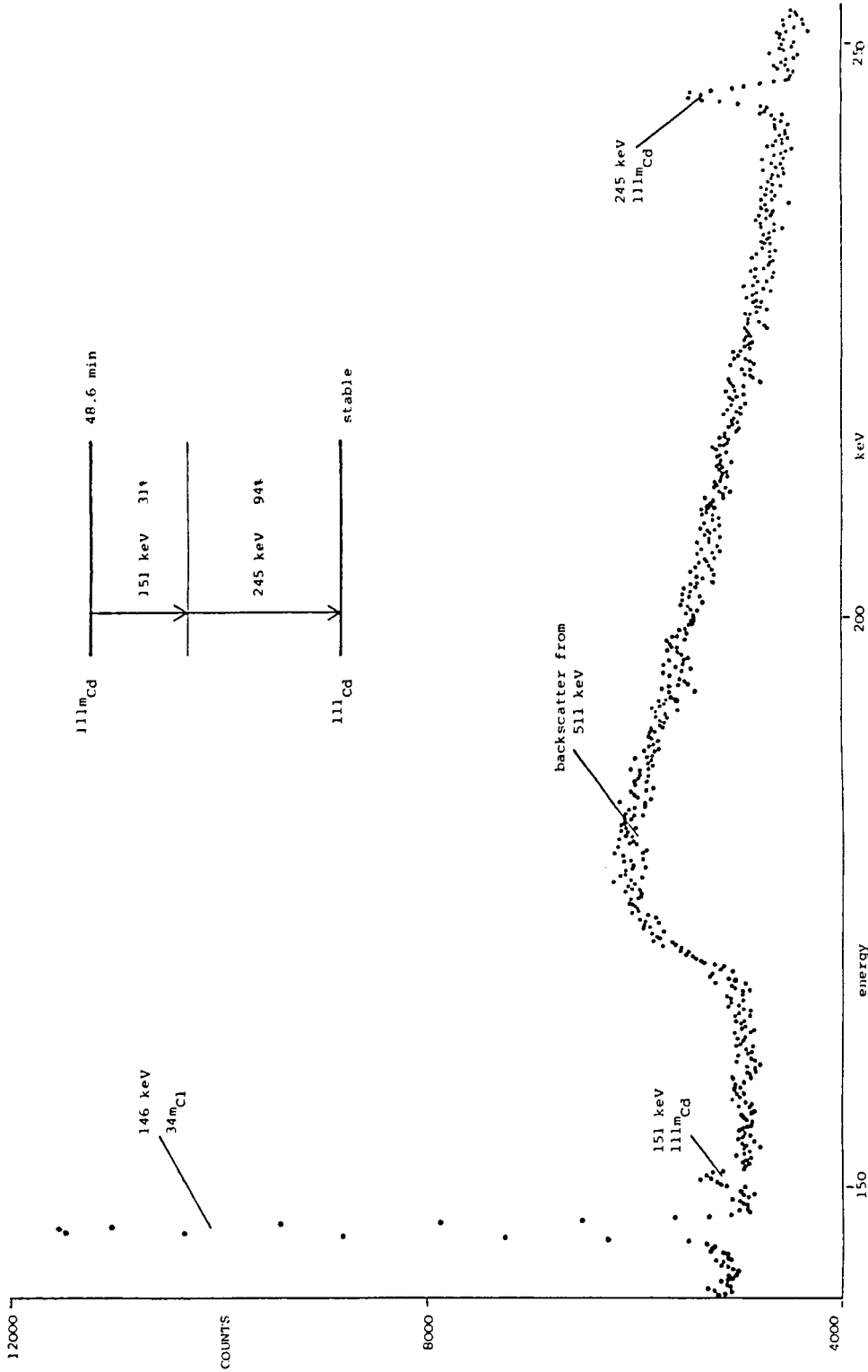


Fig. 12.  $\gamma$ -Ray energy spectrum from  $^{111m}\text{Cd}$ .



TABLE 1  
Comparison of In Vivo and In Vitro Results<sup>a</sup>

| Subject | Liver cadmium, $\mu\text{g/g}$ |                | Kidney cadmium, mg |                | Time between measurements |
|---------|--------------------------------|----------------|--------------------|----------------|---------------------------|
|         | In vivo                        | Autopsy        | In vivo            | Autopsy        |                           |
| 1       | 45.2 $\pm$ 3.6                 | 43.4 $\pm$ 6.3 | 17.1 $\pm$ 2.2     | 13.2 $\pm$ 5.3 | 2 mo                      |
| 2       | -3.1 $\pm$ 10.9                | 10.5 $\pm$ 2.9 | 4.9 $\pm$ 3.3      | 7.8 $\pm$ 0.9  | 4 yr                      |
| 3       | 47.1 $\pm$ 3.7                 | 76.5 $\pm$ 2.3 | 26.5 $\pm$ 3.3     | 14.2 $\pm$ 0.8 | 1 yr                      |

<sup>a</sup>Errors shown are from counting statistics alone; positional uncertainties are estimated to be  $\pm 20\%$  and  $\pm 25\%$  for in vivo liver and kidney measurements, respectively, and  $\pm 15\%$  for in vitro measurements.

nent feature, other than the  $^{111\text{m}}\text{Cd}$  peaks, at 146 keV is from  $^{34\text{m}}\text{Cl}$ , produced by the reaction:  $^{35}\text{Cl}(n,2n)^{34\text{m}}\text{Cl}$ . The data from those samples for which both in vitro and in vivo measurements have been made are summarized in Table 1, in which the in vivo measurements have been corrected for position. The uncertainties shown are those resulting only from counting statistics. As can be seen, the measurements are in broad general agreement, but the last set of data shows significant differences between in vivo and in vitro measurements, and, although this person had clearly been exposed to significant quantities of cadmium, his case probably does serve to emphasize the desirability of improving the accuracy associated with organ positioning.

## ACKNOWLEDGMENTS

These projects are supported by the Health and Safety Executive under contract nos. 1/MS/126/546/84 and 1/MS/126/236/80; this support and collaboration is gratefully acknowledged. DRC was able to present this paper through travel grants from the Wellcome Trust and the Royal Society.

## REFERENCES

1. L. Ahlgren, K. Liden, S. Mattsson, and S. Tejning, *Scand. J. Work Environ. Health* **2**, 82 (1976).
2. J. O. Christoffersson, A. Schütz, L. Ahlgren, B. Haeger-Aronsen, S. Mattsson, and S. Skerfving, *Am. J. Industr. Med.* **6**, 447 (1984).
3. P. Bloch, G. Garavaglia, G. Mitchell, and I. M. Shapiro, *Phys. Med. Biol.* **22**, 56 (1977).
4. J. Price, H. Baddeley, J. A. Kenardy, B. J. Thomas, and B. W. Thomas, *Br. J. Radiol.* **57**, 29 (1984).
5. L. Wielopolski, J. F. Rosen, D. N. Slatkin, D. Vartsky, K. J. Ellis, and S. H. Cohn, *Med. Phys.* **10**, 248 (1983).
6. E. E. Laird, D. R. Chettle, and M. C. Scott, *Nucl. Instrum. Meth.* **193**, 377 (1982).

7. L. J. Somervaille, E. E. Laird, D. R. Chettle, and M. C. Scott, *Int. Conf. Heavy Metals in the Environment* **1**, 521 (1983).
8. L. J. Somervaille, D. R. Chettle, and M. C. Scott, *Phys. Med. Biol.* **30**, 929 (1985).
9. J. H. Hubbell and I. Øverbø, *J. Phys. Chem. Ref. Data* **8**, 69 (1979).
10. L. J. Somervaille, Ph.D. Thesis, Department of Physics, University of Birmingham, England (1984).
11. P. S. I. Barry, in *The Biogeochemistry of Lead in the Environment*, part B, J. O. Nriagu, ed., Elsevier/North Holland, Amsterdam, 1978, pp. 97–150.
12. L. E. Wittmers, A. Alich, and A. C. Aufderheide, *Am. J. Clin. Pathol.* **75**, 80 (1981).
13. A. C. Aufderheide, F. D. Neiman, L. E. Wittmers, and G. Rapp, *Am. J. Phys. Anthropol.* **55**, 285 (1981).
14. H. C. Biggin, N. S. Chen, K. V. Ettinger, J. H. Fremlin, W. D. Morgan, R. Nowotny, and M. J. Chamberlain, *Nature New Biol.* **236**, 187 (1972).
15. J. S. McLellan, B. J. Thomas, J. H. Fremlin, and T. C. Harvey, *Phys. Med. Biol.* **20**, 88 (1975).
16. D. Vartsky, K. J. Ellis, N. S. Chen, and S. H. Cohn, *Phys. Med. Biol.* **22**, 1085 (1977).
17. K. Al-Hiti, S. Slaibi, and T. Al-Kayat, *Int. J. Appl. Rad. Isot.* **30**, 55 (1979).
18. P. E. Cummins, J. Dutton, C. J. Evans, W. D. Morgan, and A. Sivyver, *J. Radioanalyt. Chem.* **71**, 561 (1982).
19. J. B. Krauel, M. A. Speed, B. W. Thomas, H. Baddeley, and B. J. Thomas, *Int. J. Appl. Rad. Isot.* **31**, 101 (1980).
20. K. G. McNeill, J. S. McLellan, A. K. Mohammad Amin, K. Vohra and J. R. Mernagh, *J. Radioanalyt. Chem.* **71**, 573 (1982).
21. L. Ahlgren and S. Mattsson, *Phys. Med. Biol.* **26**, 19 (1981).
22. J-O. Christoffersson and S. Mattsson, *Phys. Med. Biol.* **28**, 1135 (1983).
23. I. K. Al-Haddad, D. R. Chettle, J. H. Fremlin, and T. C. Harvey. *J. Radioanalyt. Chem.* **53**, 203 (1979).
24. B. J. Thomas, T. C. Harvey, D. R. Chettle, J. S. McLellan, and J. H. Fremlin, *Phys. Med. Biol.* **24**, 432 (1979).
25. I. K. Al-Haddad, D. R. Chettle, J. G. Fletcher, and J. H. Fremlin, *Int. J. Appl. Rad. Isot.* **32**, 109 (1981).
26. M. C. Scott, D. R. Chettle, S. A. Coward, M. J. Faddy, and J. G. Fletcher, *Trans. Am. Nucl. Soc.* **44**, 33 (1983).
27. D. W. Marquardt, *J. Soc. Indust. Appl. Math.* **11**, 431 (1963).
28. P. R. Bevington, *Data Reduction and Error Analysis for the Physical Sciences*, McGraw Hill, New York, 1969.
29. W. D. Morgan, K. J. Ellis, D. Vartsky, S. Yasumura, and S. H. Cohn, *Phys. Med. Biol.* **26**, 577 (1981).
30. I. K. Al-Haddad, Ph.D. Thesis, Department of Physics, University of Birmingham, England (1979).